Arabian Journal of Chemistry (2022) **15**, 104019

King Saud University

Arabian Journal of Chemistry

www.ksu.edu.sa
www.sciencedirect.com

ORIGINAL ARTICLE

Design, synthesis, biological activity evaluation and mechanism of action of myricetin derivatives containing thioether quinazolinone

Tingting Liu [a,1], Feng Peng [a,1], Yunying Zhu [b], Xiao Cao [a], Qifan Wang [a], Fang Liu [a], Liwei Liu [a], Wei Xue [a,*]

[a] *State Key Laboratory Breeding Base of Green Pesticide and Agricultural Bioengineering, Key Laboratory of Green Pesticide and Agricultural Bioengineering, Ministry of Education, Research and Development Center for Fine Chemicals, Guizhou University, Guiyang 550025, China*
[b] *School of Chemical Engineering, Guizhou Institute of Technology, Guiyang 550001, China*

Received 11 April 2022; accepted 25 May 2022
Available online 31 May 2022

KEYWORDS

Myricetin;
Quinazolinone;
Antibacterial;
Antiviral;
TMV CP;
Chlorophyll content;
Defensive enzyme activities

Abstract Plant bacteria and viruses have a huge negative impact on food crops in the world. Therefore, it is important to create new and efficient green pesticides. In this paper, a series of myricetin derivatives containing quinazolinone sulfide were introduced. Good antibacterial and antiviral activities of the drug molecules 2-((3-((5,7-dimethoxy-4-oxo-2-(3,4,5-trimethoxyphenyl)-4*H*-chromen-3-yl)oxy)propyl)thio)-6-fluoro-3-phenylquinazolin-4(3*H*)-one (**T5**) and 2-((4-((5,7-dimethoxy-4-oxo-2-(3,4,5-trimethoxyphenyl)-4*H*-chromen-3-yl)oxy)butyl)thio)-6-methyl-3-phenylquinazolin-4(3*H*)-one (**T15**) respectively were found by biological activity screening. The value of dissociation constant (K_d) of compound **T15** to TMV CP was 0.024 ± 0.006 μM, determined by Microscale thermophoresis (MST), which was far less than the value of 8.491 ± 2.027 μM of commercial drug ningnanmycin (NNM). The interaction between compound **T15** and TMV CP was further verified by molecular docking. Compound **T15** formed strong hydrogen bonds with residues SER:49 and SER:15 (1.92 Å, 2.20 Å, respectively), which were superior to the traditional hydrogen bonds formed by NNM with residue SER:215 (3.64 Å). In addition, the effects of compound **T15** on the contents of chlorophyll and peroxidase (POD) in tobacco were studied, and the results indicated that compound **T15** could enhance the disease resistance of tobacco plants to a certain extent.

* Corresponding author.
E-mail address: wxue@gzu.edu.cn (W. Xue).
[1] Contributed equally to this work.

Peer review under responsibility of King Saud University.

Production and hosting by Elsevier

1. Introduction

Bacteria and viruses are the two major pathogens of plant, which cause huge losses in crop yields worldwide due to their extremely high infectivity and wide host-range (Li et al., 2016; Kashyap et al., 2017; Shasmita et al., 2019; Cai et al.,

https://doi.org/10.1016/j.arabjc.2022.104019
1878-5352

2020; Abdullahi et al., 2020). However, conventional chemicals used to control plant bacteria and viruses, such as bismerthiazol (BT), thiodiazole-copper (TC), ningnanmycin (NNM), have led to increasing resistance of plant pathogens due to large-scale single use. Moreover, traditional chemicals are being eliminated from the market gradually, due to their high phytotoxicity, great environmental damage, excessive pesticide residues, and difficulty in degradation (Buttimer, et al., 2017; Ren, et al., 2020; Wu, et al., 2021; Singh, et al.,2021). In recent years, with the transition of pesticide development to the green and safe direction, plant-derived pesticides became one of the third generational pesticide sources that are highly valued at home and abroad because of their advantages.

Myricetin is a polyhydroxy flavonol, extracted from the bark of myricaceae (Myricaceae) plant, also exists in various edible plants such as grapes, rattan tea, and buckwheat (Miean, et al., 2001; Kalinova, et al., 2009). A number of research results have shown that myricetin has various pharmacological activities such as antioxidant, anti-tumor, and anti-inflammatory, is a very important natural lead compound in the development of drugs and cosmetics (Mendes, et al., 2018; Mendes, et al., 2019; Sun, et al., 2019; Chobot, et al., 2020; Akhtar, et al., 2021). In recent years, with the aggravation of plant diseases, more and more pesticide researchers have turned their attention to the direction of natural products. Existing research results show that myricetin as a lead compound after structural modification have various biological activities such as antiviral and antibacterial, which opens up a new research direction to find more efficient and environmentally friendly botanical pesticides (Jiang, et al., 2020a; He, et al., 2021; Liu, et al., 2021; Peng, et al., 2021). The structures of these compounds are shown in Fig. 1.

Quinazolin-4(3*H*)-one, also known as 4-hydroxyquinazoline, is a series of nitrogen-containing heterocyclic compounds, exists widely in natural alkaloids (Al-Amiery, et al., 2014; Mahdavi, et al., 2016). In early studies, quinazolin-4(3*H*)-one and its derivatives exhibited various pharmacological activities such as antioxidant, antibacterial, and antitumor, and were the main active groups in various drug structures (Nanthakumar, et al., 2014; Rakesh, et al., 2019; Soliman, et al., 2020; Huang, et al., 2020). Recently, quinazolin-4(3*H*)-one and its derivatives have shown good antibacterial and antiviral activities in the research reports of pesticide creation for many times, so they have attracted the attention of scholars (Zu, et al., 2020; Hao, et al., 2020; Liu, et al., 2021; Peng, et al., 2021). The structures of these compounds are shown in Fig. 2.

In this article, we introduced quinazolinone, as an active group existing in natural product Febrifugine and antibacterial agent Proquinazid, into the structure of myricetin, and synthesized a series of myricetin derivatives containing thioether quinazolinone. The design idea of the target compounds is shown in Fig. 3. The target compounds with better activity were screened out through the tests of antibacterial and antiviral activities. Experiments, such as scanning electron microscope, microscale thermophoresis, molecular docking, and determination of chlorophyll and defense enzyme content, were used to preliminarily explore the mechanism of action of the compounds, in order to find highly active antibacterial and antiviral drugs.

2. Materials and methods

2.1. Instruments and chemicals

The target compounds were characterized, by using JEOL-ECX500 nuclear magnetic resonance spectrometer (Tokyo, Japan) and Thermo Scientic Q Exactive mass spectrometer (Missour, America). The K_d values of compounds to TMV CP were determined by using NanoTemper Monolith NT.115 microscale thermophoresis instrument (München, Germany). All solvents were purchased from Tianjin Zhi Yuan Regent Co., Ltd. (Tianjin, China). All reagents were purchased from Shanghai Titan chemical Co., Ltd. (Shanghai, China) and Adamas Reagent, Ltd. (Shanghai, China). Enzyme activity kits were purchased from Suzhou Keming Biotechnology Co., Ltd (Jiangsu, China).

2.2. Synthesis

2.2.1. General synthesis procedure for intermediates *1* and *2*

Intermediates **1** and **2** were synthesized with the method described in the references (Xue et al., 2015; Jiang, et al., 2020b; Li, et al; 2019).

2.2.2. General synthesis procedure for intermediate *3*

Intermediate **3** was synthesized according to previous literature (Ran, et al., 2020). Substituted benzoic acid (13.23 mmol), absolute ethanol (20 mL), substituted phenyl isothiocyanate (13.23 mmol) and triethylamine (14.55 mmol) were added to the reaction flask in sequence. After heating and stirring to reflux for 4–6 h, a white solid was precipitated. The reaction system was filtered under reduced pressure, and the filter cake was washed with a small amount of ethanol to obtain the crude product of Intermediate **3**, which was directly put into the next step after drying without purification.

2.2.3. General synthesis of target compounds *T1 – T25*

As shown in Scheme 1, the target compounds **T1 – T25** were synthesized with the method, which had been modified by us later, from the literature (Hagar, et al., 2016). Intermediate **2** (1.96 mmol), intermediate **3** (2.36 mmol), and K_2CO_3 (3.93 mmol) were added to 20 mL of DMF, reacted at 90 ℃ for 6 h. The reaction system was poured into 500 mL of ice water, and a white solid was precipitated. After being held stationarily for 2 h, it was filtered under reduced pressure and dried to obtain a crude product, which was separated and purified by column chromatography later (ethyl acetate: petroleum ether = 2:1, v/v).

2.3. Biological assays

2.3.1. Evaluation of antibacterial activity in vitro

According to the reports in the literature, the antibacterial activity of the compounds **T1 – T25** were tested by the turbidimetric assays. (Xiang, et al., 2020). The bacteria used were *Xanthomonas axonopodis pv. citri* (*Xac*) and *Xanthomonas oryzae pv.oryzae* (*Xoo*). Commercially available BT and TC were used as control agents. Methylated myricetin was used as the

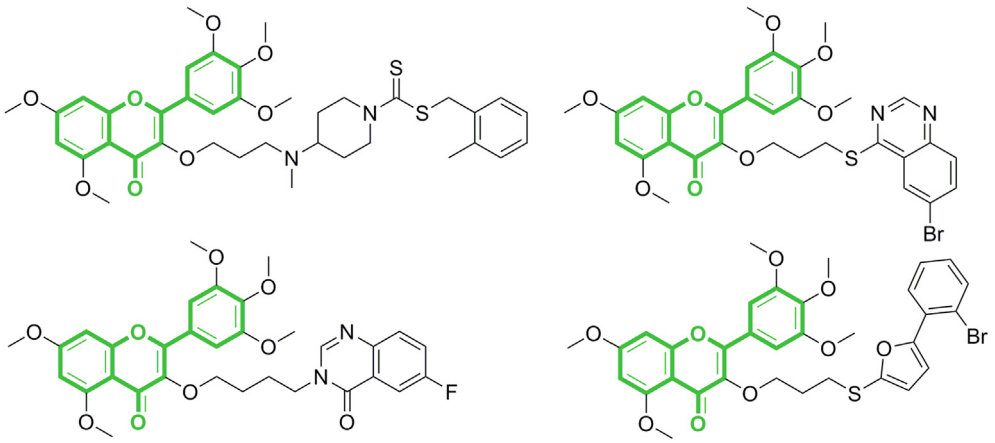

Fig. 1 Structures of myricetin derivatives previously reported by our group.

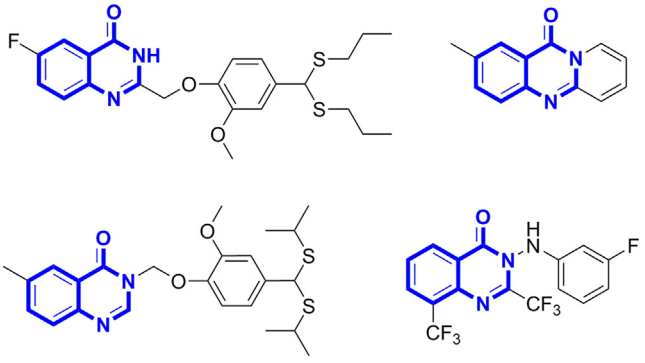

Fig. 2 Structures of quinazolinone derivatives with antiviral and antibacterial activities.

lead compound for the comparison of antibacterial activity. The corresponding concentration of DMSO solution served as a negative control. Three parallel experiments were performed for each sample.

2.3.2. Evaluation of antiviral activity in vivo

The antiviral activity of compounds **T1** – **T25** were tested with the half-leaf blight spot methods. (Chen, et al., 2019; Zhang, et al., 2021). During the experiment, DMSO was used as the solvent, and Tween-20 was used as the co-solvent. NNM was used as the control drug. Methylated myricetin was used as the lead compound for activity comparison. Three parallel experiments were performed for each sample.

2.4. Microscale thermophoresis experiment

The K_d values of some target compounds and NNM to TMV CP were determined with the method reported in the literature. (Li et al., 2019; Wu, et al., 2021). DMSO-dissolved drug was formulated into 16 concentration gradients at room temperature. Compounds were tested for K_d values on NanoTemper Monolith NT.115 after adding equal amounts of TMV CP to groups of each concentration.

2.5. Molecular docking

Molecular docking is a process in which receptors and substrates recognize each other through energy matching and geometric matching. Molecular docking is very important in both supramolecular architecture and drug design (José, et al., 2020; Gabriel, et al., 2021). The molecular docking of compound **T15** and NNM to TMV CP were carried out with the method reported in the literature (Chen, et al., 2021). Molecular docking of the TMV CP (PDB code: 1EI7) with the structure of the selected compound was performed on Discovery Studio.

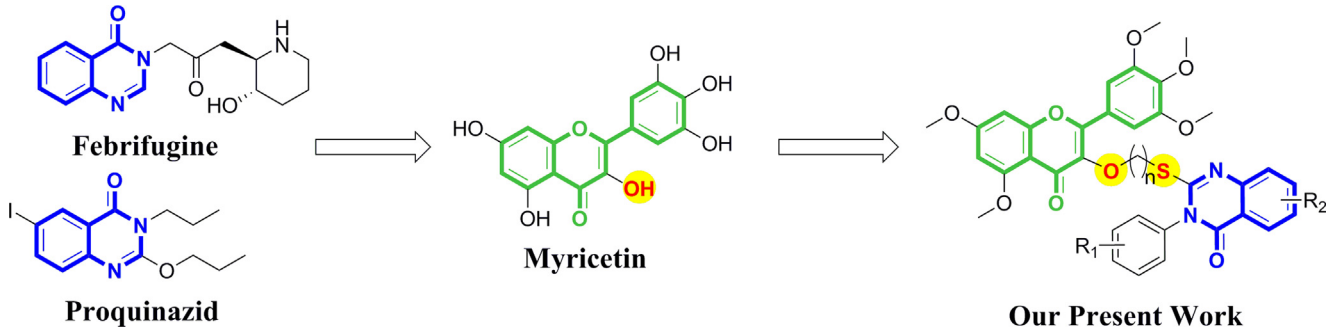

Fig. 3 Design idea for target compounds (Febrifugine and Proquinazid are two commercial antibacterial agents that contain quinazolinone groups).

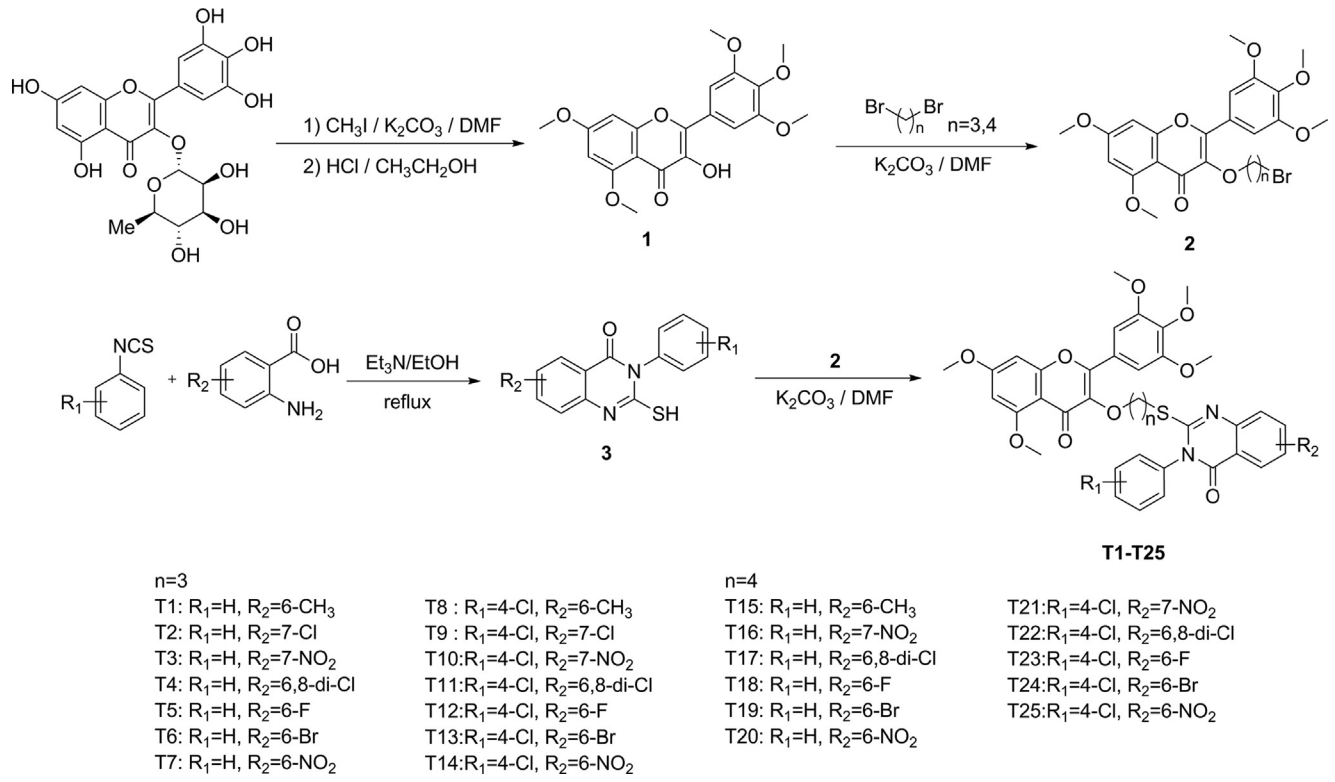

n=3

T1: R_1=H, R_2=6-CH_3
T2: R_1=H, R_2=7-Cl
T3: R_1=H, R_2=7-NO_2
T4: R_1=H, R_2=6,8-di-Cl
T5: R_1=H, R_2=6-F
T6: R_1=H, R_2=6-Br
T7: R_1=H, R_2=6-NO_2
T8 : R_1=4-Cl, R_2=6-CH_3
T9 : R_1=4-Cl, R_2=7-Cl
T10:R_1=4-Cl, R_2=7-NO_2
T11:R_1=4-Cl, R_2=6,8-di-Cl
T12:R_1=4-Cl, R_2=6-F
T13:R_1=4-Cl, R_2=6-Br
T14:R_1=4-Cl, R_2=6-NO_2

n=4

T15: R_1=H, R_2=6-CH_3
T16: R_1=H, R_2=7-NO_2
T17: R_1=H, R_2=6,8-di-Cl
T18: R_1=H, R_2=6-F
T19: R_1=H, R_2=6-Br
T20: R_1=H, R_2=6-NO_2
T21:R_1=4-Cl, R_2=7-NO_2
T22:R_1=4-Cl, R_2=6,8-di-Cl
T23:R_1=4-Cl, R_2=6-F
T24:R_1=4-Cl, R_2=6-Br
T25:R_1=4-Cl, R_2=6-NO_2

Scheme 1 Synthetic route of target compounds **T1** – **T25**.

2.6. Determination of chlorophyll content

According to the method in the literature, the compound **T15** with better protective activity was selected for the determination of the change of chlorophyll content (Gan, et al., 2017). The virus-inoculated tobacco leaves were ground in liquid nitrogen to pulverize. A mixed solution of ethanol and acetone was added and allowed to be held stationarily for 1 h in the dark. The absorbance at 645 nm and 663 nm were measured separately. The chlorophyll content was calculated according to the following formula.

$$C_a(mg/L) = 9.784OD_{663} - 0.990OD_{645}$$

$$C_b(mg/L) = 21.426OD_{645} - 4.650OD_{663}$$

$$C_t(mg/L) = C_a + C_b = 5.134OD_{663} - 20.643OD_{645}$$

$$chlorophyll\,content(mg/g) = \frac{C(mg/L) \times the\ volume\ of\ extracts(L)}{sample\ fresh\ weight(g)}$$

2.7. Determination of defense enzyme activity

Peroxidases (POD) are involved in plant development, stress responses and hormone signaling. It is closely related to the photosynthesis and respiration of plants (Wu, et al., 2019). The compound **T15** was tested for the activity of the defense enzyme according to the method in the literature (Zhou, et al., 2021). The virus-inoculated tobacco leaves were added to liquid nitrogen and ground to pulverize. The POD content of the leaves was determined with the method of enclosed instructions of testing kit.

3. Results and discussion

3.1. Structural characterization of some target compounds

2-((3-((5,7-dimethoxy-4-oxo-2-(3,4,5-trimethoxyphenyl)-4H-chromen-3-yl)oxy)propyl)thio)-6-fluoro-3-phenylquinazolin-4(3H)-one (**T5**). White solid, m.p. 185.6–187.3 °C, yield, 27%; ^{1}H NMR (500 MHz, Chloroform-*d*) δ 7.83 (dd, J = 8.1, 2.9 Hz, 1H, Ph – H), 7.55 – 7.53 (m, 1H, Ph – H), 7.53 – 7.51 (m, 3H, Ph – H), 7.41 (td, J = 8.3, 2.9 Hz, 1H, Ph – H), 7.28 (s, 2H, Ph – H), 7.28 – 7.25 (m, 2H, Ph – H), 6.48 (d, J = 2.2 Hz, 1H, Ph – H), 6.34 (d, J = 2.3 Hz, 1H, Ph – H), 4.11 (t, J = 6.2 Hz, 2H, –O – $\underline{CH_2}CH_2CH_2$ – S –), 3.95 (s, 3H, Ph – OCH_3), 3.89 (s, 3H, Ph – OCH_3), 3.88 (s, 3H, Ph – OCH_3), 3.87 (s, 6H, Ph – OCH_3), 3.26 – 3.22 (m, 2H, –O – $CH_2CH_2\underline{CH_2}$ – S –), 2.11 (p, J = 6.3 Hz, 2H, –O – $CH_2\underline{CH_2}CH_2$ – S –); ^{13}C NMR (126 MHz, Chloroform-*d*) δ 174.02, 167.85, 164.11, 161.07, 158.87, 156.67, 153.04, 152.77, 144.65, 140.48, 139.92, 135.78, 126.05, 123.24, 123.05, 120.97 (d, J = 8.4 Hz), 112.17, 111.99, 109.44, 105.85, 95.94, 92.48, 71.09, 61.11, 56.54, 56.39, 55.94, 29.73, 29.43; ^{19}F NMR (471 MHz, Chloroform-*d*) δ −114.11; HRMS (ESI) calcd for $C_{37}H_{34}O_9N_2FS$ $[M + H]^+$: 701.19636, found 701.19629.

2-((4-((5,7-dimethoxy-4-oxo-2-(3,4,5-trimethoxyphenyl)-4H-chromen-3-yl)oxy)butyl)thio)-6-methyl-3-phenylquinazolin-4(3H)-one (**T15**). White solid, m.p. 196.9–198.2 °C, yield, 56%; ^{1}H NMR (500 MHz, Chloroform-*d*) δ 7.98 (s, 1H, Ph – H), 7.53 – 7.48 (m, 4H, Ph – H), 7.45 (d, J = 8.3 Hz, 1H, Ph – H), 7.31 (s, 2H, Ph – H), 7.29 – 7.26 (m, 2H, Ph – H), 6.47 (d, J = 2.3 Hz, 1H, Ph – H), 6.33 (d, J = 2.3 Hz, 1H, Ph – H), 4.04 – 4.00 (m, 2H, –O – $\underline{CH_2}CH_2$-

Table 1 Antibacterial activities of the target compounds **T1 – T25** *in vitro*.

Compd.	*Xac*		*Xoo*	
	100 μg/mL	50 μg/mL	100 μg/mL	50 μg/mL
T1	87.8 ± 2.5	64.4 ± 1.2	40.4 ± 0.9	28.0 ± 2.3
T2	75.0 ± 3.7	52.1 ± 1.8	79.6 ± 1.9	58.6 ± 0.6
T3	59.3 ± 1.4	34.5 ± 4.0	40.6 ± 4.1	32.3 ± 6.7
T4	39.0 ± 2.2	28.9 ± 6.2	17.2 ± 3.0	14.2 ± 5.3
T5	89.1 ± 0.8	64.8 ± 1.7	82.1 ± 0.9	67.5 ± 3.2
T6	59.2 ± 2.0	40.7 ± 3.6	49.6 ± 6.8	30.2 ± 7.9
T7	31.0 ± 6.9	14.6 ± 1.4	19.5 ± 0.3	17.0 ± 4.5
T8	58.5 ± 2.3	49.2 ± 2.1	27.7 ± 1.2	18.3 ± 3.2
T9	40.6 ± 5.6	16.5 ± 4.1	24.0 ± 2.2	19.2 ± 7.2
T10	32.8 ± 1.6	18.9 ± 3.1	37.0 ± 1.9	22.0 ± 1.7
T11	47.9 ± 9.9	23.0 ± 1.7	28.5 ± 1.9	15.2 ± 3.5
T12	61.5 ± 4.8	51.7 ± 4.1	30.6 ± 4.8	16.3 ± 7.3
T13	45.2 ± 6.0	29.5 ± 3.4	28.4 ± 1.1	17.7 ± 3.2
T14	17.9 ± 8.8	9.9 ± 7.1	22.8 ± 2.1	14.0 ± 2.5
T15	68.3 ± 1.3	42.7 ± 4.6	89.1 ± 0.6	64.3 ± 0.8
T16	52.4 ± 6.0	34.8 ± 3.7	77.7 ± 1.4	64.8 ± 1.7
T17	61.2 ± 2.7	28.9 ± 5.6	27.1 ± 2.0	10.5 ± 1.7
T18	58.2 ± 0.8	36.8 ± 4.5	44.2 ± 5.8	30.3 ± 2.3
T19	68.2 ± 6.4	46.9 ± 2.7	36.9 ± 0.4	14.3 ± 4.2
T20	63.9 ± 0.7	26.7 ± 1.6	29.4 ± 3.4	15.0 ± 3.4
T21	68.6 ± 3.7	41.8 ± 1.6	24.1 ± 3.3	15.7 ± 3.2
T22	64.6 ± 1.1	53.1 ± 1.3	44.7 ± 3.1	24.3 ± 2.4
T23	56.8 ± 2.6	37.6 ± 2.8	25.2 ± 2.7	19.3 ± 0.9
T24	47.4 ± 2.6	27.2 ± 2.4	30.2 ± 2.6	17.1 ± 1.3
T25	19.9 ± 9.5	4.6 ± 1.3	17.8 ± 2.9	12.9 ± 3.6
myricetin	43.5 ± 2.0	30.3 ± 0.8	55.2 ± 1.3	37.4 ± 2.2
BT	60.2 ± 1.3	44.6 ± 1.8	54.0 ± 1.2	42.9 ± 1.1
TC	53.6 ± 0.4	36.8 ± 1.2	54.2 ± 0.7	38.0 ± 0.8

Table 2 The EC_{50} values of several target compounds against *Xac* and *Xoo*.

Bacteria	Compd.	n	R_1	R_2	Toxic Regression equation	r^2	EC_{50} (μg/mL)
Xac	**T1**	3	H	6 – CH_3	y = 1.5892x + 2.8183	0.969	23.6 ± 2.9
	T5	3	H	6 – F	y = 1.6060x + 2.8316	0.963	22.4 ± 2.1
	myricetin	–	–	–	y = 0.9290x + 2.9584	0.992	135.6 ± 2.4
	BT	–	–	–	y = 1.0215x + 3.1677	0.989	62.2 ± 2.5
	TC	–	–	–	y = 1.0219x + 2.9673	0.978	97.5 ± 1.4
Xoo	**T5**	3	H	6 – F	y = 1.1404x + 3.5541	0.974	18.5 ± 2.6
	T15	4	H	6 – CH_3	y = 1.5790x + 2.8935	0.958	21.6 ± 1.8
	myricetin	–	–	–	y = 0.7711x + 3.4838	0.949	92.5 ± 2.2
	BT	–	–	–	y = 0.7396x + 3.6657	0.959	63.7 ± 1.4
	TC	–	–	–	y = 1.0206x + 3.0250	0.991	86.1 ± 3.7

CH_2CH_2 – S –), 3.94 (s, 3H, Ph – OCH_3), 3.90 – 3.87 (m, 12H, Ph – OCH_3), 3.19 – 3.14 (m, 2H, –O – $CH_2CH_2CH_2$-$\underline{CH_2}$ – S –), 2.44 (s, 3H, Ph – CH_3), 1.83 (p, J = 3.0, 2.6 Hz, 4H, –O – $CH_2\underline{CH_2CH_2}CH_2$ – S –); ^{13}C NMR (126 MHz, Chloroform-*d*) δ 174.07, 164.04, 162.06, 161.09, 158.85, 156.30, 153.00, 152.60, 145.98, 140.68, 139.88, 136.21, 136.07, 135.80, 129.90, 129.71, 129.27, 126.63, 126.15, 119.58, 109.47, 105.84, 95.87, 92.46, 71.82, 61.12, 56.52, 56.38, 55.92, 32.26, 29.54, 25.43, 21.35; HRMS (ESI) calcd for $C_{39}H_{39}O_9N_2S$ $[M + H]^+$: 711.23708, found 711.23706.

3.2. Antibacterial activity of the target compounds ***T1 – T25***

The results of Table 1 show that most of the compounds had a certain inhibitory effect on *Xac* and *Xoo* when the concentration of compound was 100 μg/mL. In particular, compounds **T1** and **T5** exhibited good inhibitory activity against *Xac*, with the inhibition rates of 87.8 and 89.1% respectively, which were superior than those of commercial drugs BC (60.2 %) and TC (53.6 %). The inhibitory activity against *Xoo* of compounds **T2**, **T5**, **T15** and **T16**, with inhibition rates of 79.6, 82.1, 89.1

Table 3 Antiviral activities of the target compounds **T1** – **T25** against TMV *in vivo*.

Compd.	n	R_1	R_2	Curative (%)	Protective (%)	Inactivating (%)
T1	3	H	6 – CH3	42.9 ± 2.7	29.6 ± 2.5	47.1 ± 6.7
T2	3	H	7 – Cl	68.1 ± 4.2	64.3 ± 2.1	61.3 ± 3.9
T3	3	H	7 – NO2	40.9 ± 2.6	46.3 ± 2.7	59.4 ± 2.0
T4	3	H	6,8 – di – Cl	40.8 ± 3.4	57.1 ± 4.6	46.1 ± 5.7
T5	3	H	6 – F	46.5 ± 3.4	57.6 ± 4.1	63.8 ± 3.0
T6	3	H	6 – Br	55.8 ± 6.8	44.8 ± 5.1	48.6 ± 7.6
T7	3	H	6 – NO_2	50.7 ± 1.9	44.4 ± 6.1	60.4 ± 7.1
T8	3	4 – Cl	6 – CH_3	53.7 ± 2.9	48.9 ± 4.9	43.1 ± 3.0
T9	3	4 – Cl	7 – Cl	51.2 ± 3.5	31.1 ± 4.1	53.5 ± 7.2
T10	3	4 – Cl	7 – NO_2	49.9 ± 2.6	48.3 ± 2.4	43.2 ± 3.6
T11	3	4 – Cl	6,8 – di – Cl	59.4 ± 7.1	68.2 ± 4.7	68.8 ± 9.0
T12	3	4 – Cl	6 – F	28.1 ± 3.0	44.5 ± 5.2	56.0 ± 3.3
T13	3	4 – Cl	6 – Br	44.1 ± 2.1	47.3 ± 2.8	52.9 ± 5.7
T14	3	4 – Cl	6 – NO_2	49.3 ± 4.5	48.5 ± 3.5	35.6 ± 2.2
T15	4	H	6 – CH_3	67.3 ± 2.8	64.3 ± 4.3	64.6 ± 6.7
T16	4	H	7 – NO_2	25.4 ± 8.9	39.2 ± 5.6	32.4 ± 6.7
T17	4	H	6,8 – di – Cl	44.4 ± 3.3	58.9 ± 2.3	54.2 ± 6.4
T18	4	H	6 – F	42.4 ± 1.9	28.1 ± 4.1	57.8 ± 2.9
T19	4	H	6 – Br	47.1 ± 4.6	49.2 ± 5.4	66.7 ± 7.8
T20	4	H	6 – NO_2	57.3 ± 5.8	43.8 ± 3.1	41.8 ± 1.8
T21	4	4 – Cl	7 – NO_2	43.1 ± 5.8	48.4 ± 2.9	41.3 ± 2.4
T22	4	4 – Cl	6,8 – di – Cl	55.6 ± 2.4	37.6 ± 2.2	58.2 ± 1.8
T23	4	4 – Cl	6 – F	30.6 ± 3.1	51.7 ± 3.4	22.4 ± 3.1
T24	4	4 – Cl	6 – Br	52.3 ± 5.6	43.0 ± 1.9	48.5 ± 4.5
T25	4	4 – Cl	6 – NO_2	51.8 ± 4.6	49.6 ± 1.7	64.3 ± 4.1
myricetin	–	–	–	36.7 ± 2.6	45.6 ± 3.9	43.4 ± 2.3
NNM	–	–	–	54.1 ± 2.1	57.1 ± 1.9	85.3 ± 3.8

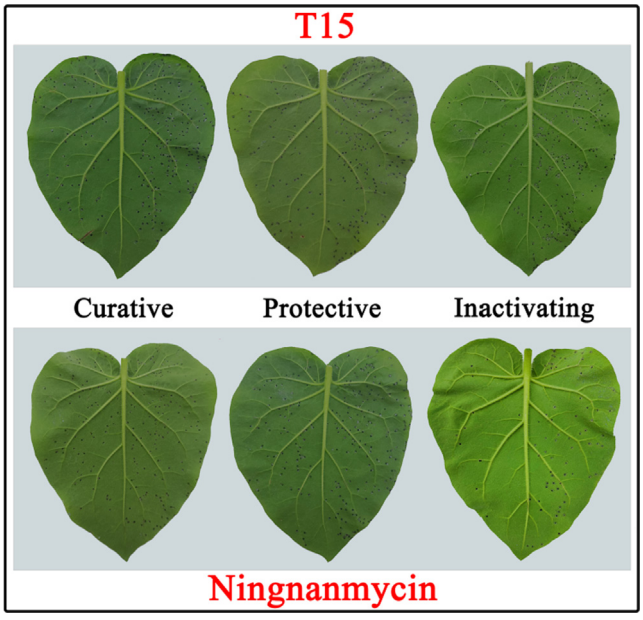

Fig. 4 Tobacco leaf morphology effects of **T15** and NNM against TMV *in vivo*. The left side of each leaf was drug-treated, the right side of each leaf was untreated with drug.

and 77.7% respectively, had better advantages than those of BT (54.0%) and TC (54.2%).

Based on the activity screening results, the EC_{50} values of some target compounds were tested, whose results are displayed in Table 2. The EC_{50} values of compounds **T1** and **T5** against *Xac* were 23.6 and 22.4 μg/mL respectively, which were less than the control drugs BT (62.2 μg/mL) and TC (97.5 μg/mL). The EC_{50} values of compounds **T5** and **T15** against *Xoo* were 18.5 and 21.6 μg/mL respectively, which were much better than BT (63.7 μg/mL) and TC (86.1 μg/mL). In particular, compound **T5** has good inhibitory activity against both plant bacteria.

*3.3. Antiviral activity of the target compounds **T1** – **T25***

The test results of antiviral activity of the target compounds **T1** – **T25** are shown in Table 3. When the compound concentration was 500 μg/mL, compounds **T2** and **T15** had good curative activity against TMV, and the inhibition rates were 68.1 and 67.3% respectively, which were higher than the commercial drug NNM (54.1%). The protective activity against TMV of compounds **T2**, **T11** and **T15**, with the inhibition rates of 64.3, 68.2 and 64.3 % respectively, were better than the commercial drug NNM (57.1%). Fig. 4 reveals the morphology of compound **T15** against TMV *in vivo*.

The EC_{50} values of compounds **T2**, **T11, T15** and NNM are summarized in Table 4. Compounds **T2**, **T11** and **T15** have good curative activity against TMV, with EC_{50} values of 190.0, 227.3 and 166.9 μg/mL respectively, which were lower than the commercial drug NNM of 319.7 μg/mL. In terms of protective activity, the EC_{50} values of compounds **T2**, **T11** and **T15** against TMV were 228.7, 178.9 and 130.5 μg/mL respectively, which were lower than NNM (341.3 μg/mL).

Table 4 The EC_{50} values of several target compounds and ningnanmycin against TMV.

	Compd.	n	R_1	R_2	Regression equation	r^2	EC_{50} (μg/mL)
Curative	**T2**	3	H	7 – Cl	y = 1.0787x + 2.5418	0.998	190.0 ± 3.4
	T11	3	4 – Cl	6,8 – di – Cl	y = 0.7626x + 3.2028	0.982	227.3 ± 2.7
	T15	4	H	6 – CH_3	y = 0.8419x + 3.1289	0.989	166.9 ± 2.1
	NNM	–	–	–	y = 0.6087x + 3.4754	0.998	319.7 ± 4.7
Protective	**T2**	3	H	7 – Cl	y = 1.2654x + 2.0146	0.962	228.7 ± 2.3
	T11	3	4 – Cl	6,8 – di – Cl	y = 0.9593x + 2.8390	0.942	178.9 ± 3.2
	T15	4	H	6 – CH_3	y = 0.7412x + 3.4319	0.966	130.5 ± 4.8
	NNM	–	–	–	y = 0.9198x + 2.6743	0.962	341.3 ± 3.9

3.4. Structure-activity relationship

Referring to the previous research reports on quinazolinones, most of the changes of substituents are carried out at the 6-position. In addition, electron withdrawing groups were often used as substituents. (Zu, et al., 2021). From the results of antibacterial activity, the compounds with – CH_3 and – F at the 6th substitution position have better antibacterial activity. For example, compounds **T1**, **T5** and **T15** exhibited inhibitory activities more than 80% on *Xac* and *Xoo* at the tested concentration of 100 μg/mL. The results of antiviral activity showed that some compounds containing – Cl and – CH_3 had better inhibitory activity on TMV. Compared with the previously reported compounds (Liu, et al., 2021), the antibacterial activity of some of the compounds with n = 3 was improved after the introduction of thioether, and the anti-TMV activity was also generally improved.

3.5. Microscale thermophoresis

The K_d value shows the affinity of the interaction between two molecules. The smaller the value is, the stronger the affinity of the two molecules is (Wang, et al., 2020). Fig. 5 shows that the binding constants (K_d) of compounds **T2**, **T11**, **T15** and NNM to TMV CP. Among them, the K_d value of compound **T15** to TMV CP was 0.024 ± 0.006 μM, which was smaller than that of compounds **T2** (0.052 ± 0.016 μM) and **T11** (0.054 ± 0.023 μM). However, the above data are extremely small compared with NNM (8.491 ± 2.027 μM). It shows that the bind-

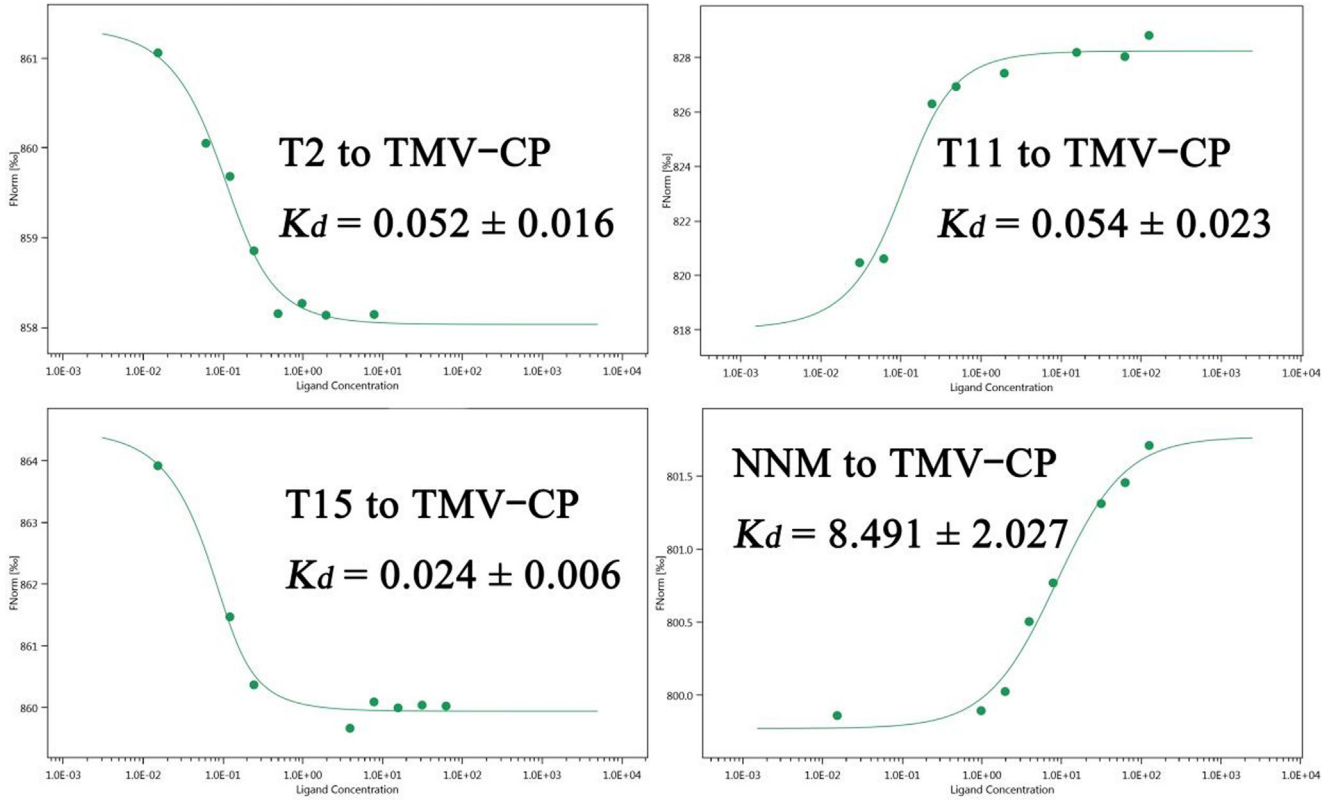

Fig. 5 The K_d values of comporids **T2**, **T11**, **T15** and NNM to TMV CP.

ing abilities of compounds **T2**, **T11** and **T15** to TMV CP are much greater than that of the control drug NNM. These results were positively correlated with EC_{50} values.

3.6. Molecular docking

The length of hydrogen bonds is negatively correlated with the binding force, and the number of hydrogen bonds is positively

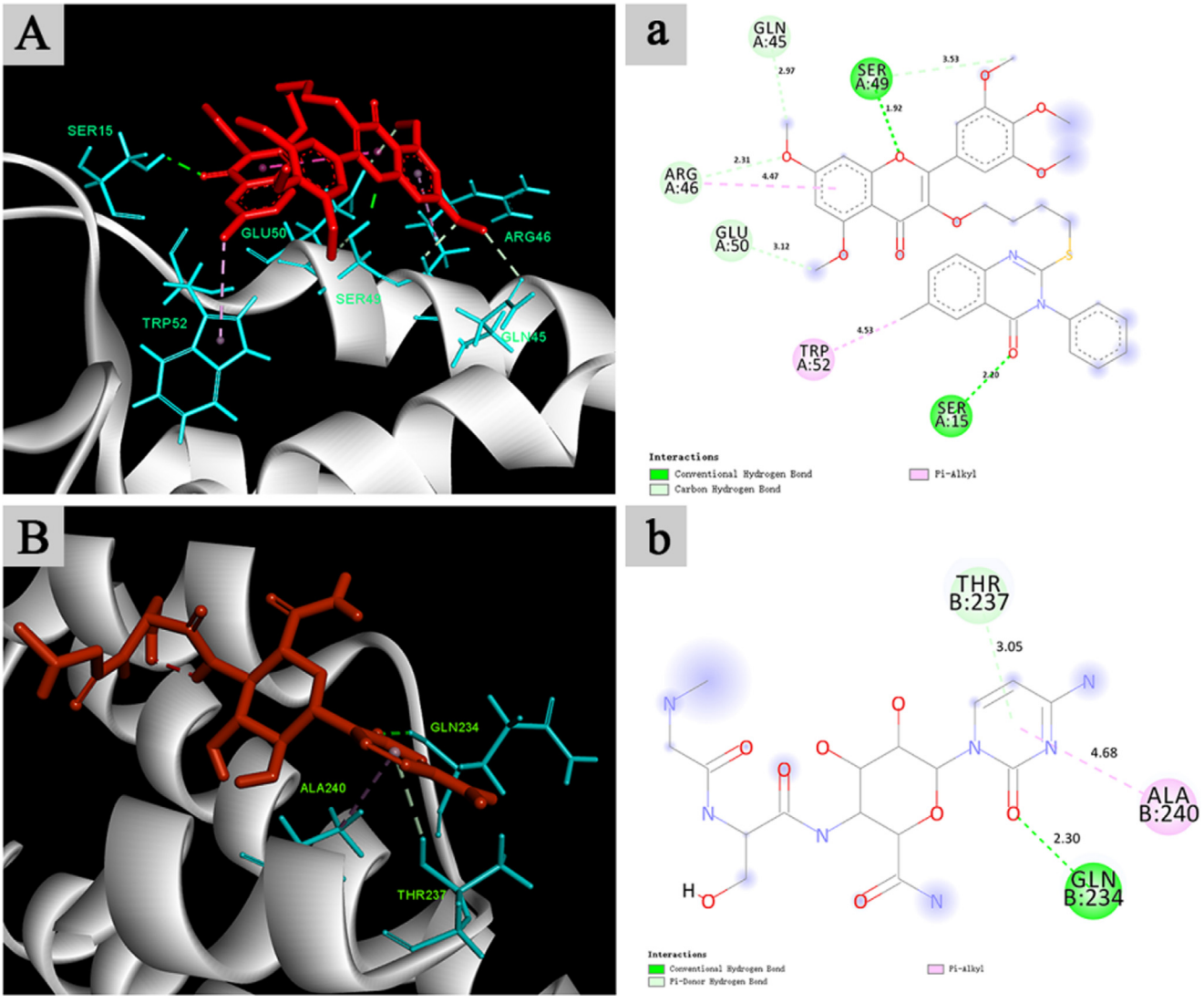

Fig. 6 Molecular docking of compound **T15** (A, a) and NNM (B, b) to TMV CP.

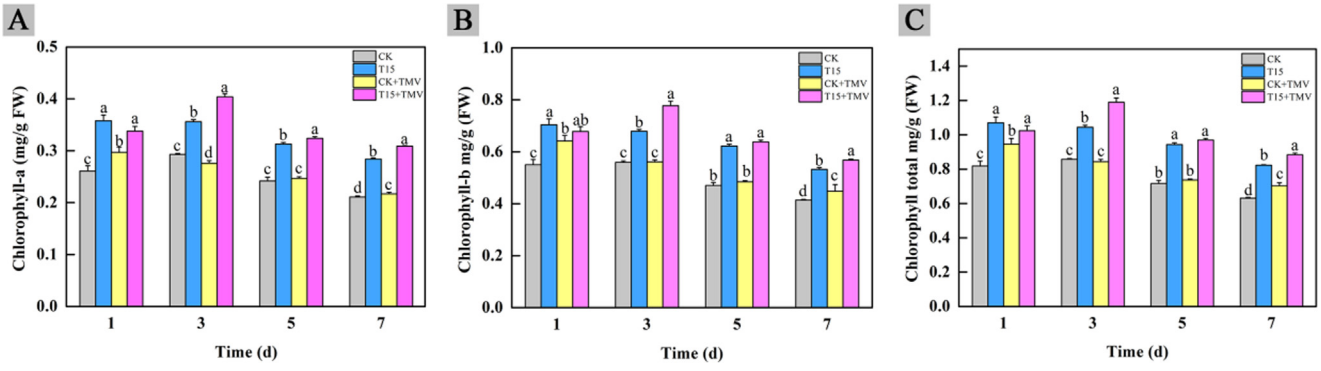

Fig. 7 Changes of chlorophyll content in tobacco after compound **T15** treatment.

correlated with the binding force (Wang, et al., 2021).The pictures in Fig. 6 validate the binding ability of the compound **T15** and NNM to TMV CP. Compound **T15** (A, a) interacted with surrounding residues SER A:49, SER A:15, ARG A:46, GLN A:45, GLU A:50 and TRP A:52 in the TMV CP active pocket via conventional hydrogen bond, carbon hydrogen interacts with π-alkyl. Compound **T15** formed two strong hydrogen bonds with residues SER A:49 (1.92 Å) and SER A:15 (2.20 Å). The commercial drug NNM (B, b), interacted with surrounding residues THR B:237, ALA B:240 and GLN B:234 in the active pocket of TMV CP via π-donor hydrogen bond, π-alkyl and conventional hydrogen bond. The naked amino group in the NNM structure formed a traditional hydrogen bond (2.30 Å) with residue SER B:215. Based on the above analysis, it was found that compound **T15** was superior to commercial drug NNM in terms of the number of action sites and hydrogen bond length. Compared with NNM, **T15** has a stronger binding ability than that of TMV CP, which has the potential for being a more effective antiviral agent.

*3.7. Effects of compound **T15** on chlorophyll content in tobacco*

Chlorophyll is an important substance for plants to carry out photosynthesis. It is reported that plant diseases induce a decrease in chlorophyll content in plants, resulting in reduced crop yields (Mandal, et al., 2009). The following conclusions could be drawn from Fig. 7: firstly, the chlorophyll content in CK group increased slightly on the third day, but decreased gradually in the later period as time went by. Secondly, CK + TMV group showed a slight increase in chlorophyll content after the TMV inoculation on first day, followed by a decreasing trend. Thirdly, the chlorophyll content in **T15** group increased significantly on the first day after TMV inoculation, and decreased in the later period. Finally, the overall change trend of the **T15** + TMV group was similar to that of the CK group, but its chlorophyll content increased significantly on the third day, which showed that the compound **T15** caused the chlorophyll content in the plant to reach its peak at this time, and the chlorophyll content gradually decreased with plant aging at a later stage.

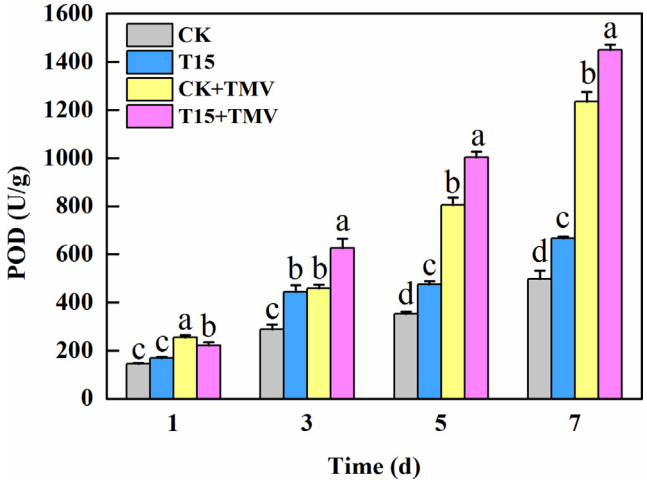

Fig. 8 Effects of compound **T15** on POD content in tobacco.

*3.8. Effects of compound **T15** on peroxidase (POD) content in tobacco*

The elevated POD content helps to scavenge free radicals in plants to improve disease resistance (Gan, et al., 2021). The changes in peroxidase (POD) content in tobacco after treatment with compound **T15** are displayed in Fig. 8. The POD content of each group gradually increased over time during the 7 d of TMV inoculation. In general, POD content in CK + TMV and **T15** + TMV groups increased significantly on the fifth and seventh days compared with CK and **T15** groups. In addition, POD contents of **T15** group and **T15** + TMV group were higher than that of group without compound **T15** treatment. The above analysis showed that compound **T15** could make peroxidase increase to a certain extent and enhance plant disease resistance.

4. Conclusions

In summary, myricetin derivatives containing thioether quinazolinone have antibacterial and anti-TMV activity. Compounds **T2**, **T11** and **T15** even surpassed the commercial drug NNM in terms of curative and protective activity, which was also confirmed by their K_d values. Molecular docking proved that compound **T15** has strong binding ability to TMV CP further. Meanwhile, the results of chlorophyll and peroxidase content measurements indicated that compound **T15** enhances the disease resistance of tobacco plants, and was a potential antiviral drug molecule.

Declaration of Competing Interest

The authors declare that they have no known competing financial interests or personal relationships that could have appeared to influence the work reported in this paper.

Acknowledgements

This research was completed with the support of the National Natural Science Foundation of China (No. 21867003), the Science Foundation of Guizhou Province (No. 20192452), Natural Science research project of Guizhou Education Department (No. 2018009), Science and Technology Program of Guizhou Province (No. 20191139), the Young Science and Technology Talents Development Program of Education Department of Guizhou Province (No. 2018251).

Appendix A. Supplementary material

Supplementary data to this article can be found online at https://doi.org/10.1016/j.arabjc.2022.104019.

References

Abdullahi, A. et al, 2020. Phytochemical profiling and antimicrobial activity of ginger (Zingiber officinale) essential oils against important phytopathogens. Arab. J. Chem. 13, 8012–8025.

Akhtar, S. et al, 2021. Anticancer potential of myricetin bulk and nano forms in vitro in lymphocytes from myeloma patients. Arch. Toxicol. 95, 337–343.

Al-Amiery, A.A. et al, 2014. Antioxidant and antimicrobial activities of novel quinazolinones. Med. Chem. Res. 23, 236–242.
Buttimer, C. et al, 2017. Bacteriophages and bacterial plant diseases. Front. Microbiol. 8, 34.
Cai, L. et al, 2020. Plant-derived compounds: A potential source of drugs against Tobacco mosaic virus. Pestic. Biochem. Physiol. 169, 104589.
Chen, M. et al, 2021. Antibacterial and antiviral activities and action mechanism of flavonoid derivatives with a benzimidazole moiety. J. Saudi Chem. Soc. 25, 101194.
Chen, Z.W. et al, 2019. Synthesis, antiviral activity, and 3D-QSAR study of novel chalcone derivatives containing malonate and pyridine moieties. Arab. J. Chem. 12, 2685–2696.
Chobot, V. et al, 2020. In vitro evaluation of pro- and antioxidant effects of flavonoid tricetin in comparison to Myricetin. Molecules 25, 5850.
de Souza, G.L.C., Peterson, K.A., 2021. Benchmarking antioxidant-related properties for gallic acid through the use of DFT, MP2, CCSD, and CCSD(T) approaches. J. Phys. Chem. A 125, 198–208.
Gan, X.H. et al, 2017. Novel trans-ferulic acid derivatives containing a chalcone moiety as potential activator for plant resistance induction. J. Agric. Food Chem. 65, 4367–4377.
Gan, X.H. et al, 2021. Synthesis of novel antiviral ferulic acid−eugenol and isoeugenol hybrids using various link reactions. J. Agric. Food Chem. 69, 13724–13733.
Hagar, M. et al, 2016. Synthesis, molecular structure and spectroscopic studies of some new quinazolin-4(3*H*)-one derivatives; an account on the N- versus S-Alkylation. J. Mol. Struct. 1108, 667–679.
Hao, Y.N. et al, 2020. Luotonin A and its derivatives as novel antiviral and antiphytopathogenic fungus agents. J. Agric. Food Chem. 68, 8764–8773.
He, J. et al, 2021. Design, synthesis and biological activities of myricetin derivatives containing quinazoline thioether moiety. Chin. J. Org. Chem. 41, 708–718.
Huang, W.Y. et al, 2020. Pyridazino[1,6-b]quinazolinones as new anticancer scaffold: Synthesis, DNA intercalation, topoisomerase I inhibition and antitumor evaluation in vitro and in vivo. Bioorg. Chem. 99, 103814.
Jiang, S.C. et al, 2020a. Antibacterial activities of novel dithiocarbamate-containing 4*H*-chromen-4-one derivatives. J. Agric. Food Chem. 68, 5641–5647.
Jiang, S.C. et al, 2020b. Design, synthesis and antibacterial activities against Xanthomonas oryzae pv. oryzae, Xanthomonas axonopodis pv. citri and Ralstonia solanacearum of novel myricetin derivatives containing sulfonamide moiety. Pest Manag. Sci. 76, 853–860.
José, L.F.S. et al, 2020. Probing structural properties and antioxidant activity mechanisms for eleocarpanthraquinone. J. Mol. Model. 26, 233.
Kalinova, J., Vrchotova, N., 2009. Level of Catechin, Myricetin, Quercetin and Isoquercitrin in buckwheat (fagopyrum esculentum moench), changes of their levels during vegetation and their effect on the growth of selected weeds. J. Agric. Food Chem. 57, 2719–2725.
Kashyap, P.L. et al, 2017. Nanodiagnostics for plant pathogens. Environ. Chem. Lett. 15, 7–13.
Li, P. et al, 2019. Synthesis and biological activities of myricetin derivatives containing quinoxaline. Chem. J. Chin. Univ. 40, 909–917.
Li, X.Y. et al, 2016. New strategies and methods to study interactions between tobacco mosaic virus coat protein and its inhibitors. Int. J. Mol. Sci. 17, 252.
Li, X.Y. et al, 2019. Cucumber mosaic virus coat protein: The potential target of 1, 4-pentadien-3-one derivatives. Pestic. Biochem. Physiol. 155, 45–50.
Liu, T.T. et al, 2021. Design, synthesis, antibacterial activity, antiviral activity, and mechanism of myricetin derivatives containing a quinazolinone moiety. ACS Omega 6, 30826–30833.
Liu, Y.W. et al, 2021. First report on anti-TSWV activities of quinazolinone derivatives containing a dithioacetal moiety. J. Agric. Food Chem. 69, 12135–12142.
Mahdavi, M. et al, 2016. Synthesis of novel fused quinazolinone derivatives. Mol. Divers. 20, 677–685.
Mandal, K. et al, 2009. Effect of downy mildew disease on photosynthesis and chlorophyll fluorescence in *Plantago ovata* Forsk. J. Plant Dis. Protect. 116, 164–168.
Mendes, R.A. et al, 2018. A computational investigation on the antioxidant potential of myricetin 3,4'-di-*O*-α-*L*-rhamnopyranoside. J. Mol. Model. 24, 133.
Mendes, R.A. et al, 2019. Evaluation of the antioxidant potential of myricetin 3-*O*-α-*L*-rhamnopyranoside and myricetin 4'-*O*-α-*L*-rhamnopyranoside through a computational study. J. Mol. Model. 25, 89.
Miean, K.H., Mohamed, S., 2001. Flavonoid (Myricetin, Quercetin, Kaempferol, Luteolin, and Apigenin) content of edible tropical plants. J. Agric. Food Chem. 49, 3106–3112.
Nanthakumar, R. et al, 2014. Anti-inflammatory and antibacterial activity study of some novel quinazolinones. Arab. J. Chem. 7, 1049–1054.
Peng, F. et al, 2021. Antibacterial and antiviral activities of 1,3,4-oxadiazole thioether 4*H* -chromen-4-one derivatives. J. Agric. Food Chem. 69, 11085–11094.
Peng, J.W. et al, 2021. Design, synthesis, and structure-activity relationship of quinazolinone derivatives as potential fungicides. J. Agric. Food Chem. 69, 4604–4614.
Rakesh, K.P. et al, 2019. Anticancer and DNA binding studies of potential amino acids based quinazolinone analogs: synthesis, SAR and molecular docking. Bioorg. Chem. 87, 252–264.
Ran, L.L. et al, 2020. Discovery of potent and novel quinazolinone sulfide inhibitors with anti-ToCV activit. J. Agric. Food Chem. 68, 5302–5308.
Ren, X.L. et al, 2020. Design, synthesis, antiviral bioactivity, and mechanism of the ferulic acid ester-containing sulfonamide moiety. ACS Omega 5, 19721–19726.
Shasmita, M., D.,, et al, 2019. Priming with salicylic acid induces defense against bacterial blight disease by modulating rice plant photosystem II and antioxidant enzymes activity. Pestic. Biochem. Physiol. Physiol. Mol. Plant Pathol. 108, 101427.
Singh, N. et al, 2021. Antioxidant and antimicrobial study of Schefflera vinosa leaves crude extracts against rice pathogens. Arab. J. Chem. 14, 103243.
Soliman, A.M. et al, 2020. Antioxidant activity of novel quinazolinones bearing sulfonamide: potential radiomodulatory effects on liver tissues via NF-kB/ PON1 pathway. Eur. J. Med. Chem. 197, 112333.
Sun, F.Y. et al, 2019. New micelle myricetin formulation for ocular delivery: improved stability, solubility, and ocular anti-inflammatory treatment. Drug Deliv. 26, 575–585.
Wang, X.B. et al, 2021. Novel pyrazole-4-acetohydrazide derivatives potentially targeting fungal succinate dehydrogenase: design, synthesis, three-dimensional quantitative structure−activity relationship, and molecular docking. J. Agric. Food Chem. 69, 9557–9570.
Wang, Y.J. et al, 2020. Design, synthesis, anti-TMV activity, and preliminary mechanism of cinnamic acid derivatives containing dithioacetal moiety. Pestic. Biochem. Physiol. 164, 115–121.
Wu, C.L. et al, 2019. The class III peroxidase (POD) gene family in cassava: identification, phylogeny, duplication, and expression. Int. J. Mol. Sci. 20, 2730.
Wu, S.K. et al, 2021. Synthesis, antibacterial activity, and mechanisms of novel 6-sulfonyl-1,2,4-triazolo[3,4-b] [1,3,4] thiadiazole derivatives. J. Agric. Food Chem. 69, 4645–4654.
Wu, Z.B. et al, 2021. In vivo antiviral activity and disassembly mechanism of novel 1-phenyl-5-amine-4-pyrazole thioether derivatives against tobacco mosaic virus. Pestic. Biochem. Physiol. 173, 104771.

Xiang, J. et al, 2020. Design and synthesis of novel 1,3,4-oxadiazole sulfone compounds containing 3,4-dichloroisothiazolylamide moiety and evaluation of rice bacterial activity. Pestic. Biochem. Physiol. 170, 104695.

Xue, W. et al, 2015. Novel myricetin derivatives: design, synthesis and anticancer activity. Eur. J. Med. Chem. 97, 155–163.

Zhang, J. et al, 2021. Purine nucleoside derivatives containing a sulfa ethylamine moiety: design, synthesis, antiviral activity, and mechanism. J. Agric. Food Chem. 69, 5575–5582.

Zhou, X. et al, 2021. Design, synthesis and anti-TMV activity of novel α-aminophosphonate derivatives containing a chalcone moiety that induce resistance against plant disease and target the TMV coat protein. Pestic. Biochem. Physiol. 172, 104749.

Zu, G.C. et al, 2020. Design, synthesis, and anti-ToCV activity of novel 4(3*H*)-quinazolinone derivatives bearing dithioacetal moiety. J. Agric. Food Chem. 68, 5539–5544.

Zu, G.C. et al, 2021. Synthesis, anti-tomato spotted wilt virus activities, and interaction mechanisms of novel dithioacetal derivatives containing a 4(3*H*)-quinazolinone pyrimidine ring. J. Agric. Food Chem. 69, 14459–14466.